Available online at www.sciencedirect.com
SCIENCE DIRECT®
Spectrochimica Acta Part A 61 (2005) 109–116
SPECTROCHIMICA ACTA PART A
www.elsevier.com/locate/saa

New luminescent terbium complex for the determination of DNA

Alla Yegorova [a], Alexander Karasyov [b], Axel Duerkop [b,*], Igor Ukrainets [c], Valery Antonovich [a]

[a] AV Bogatsky Physico-Chemical Institute of the National Academy of Sciences of Ukraine, 86, Lustdorfskaya doroga, Odessa 65080, Ukraine
[b] Institute of Analytical Chemistry, Chemo- and Biosensors, University of Regensburg, Universitätsstraße 31, 93040, Regensburg, Germany
[c] National University of Pharmacy, Blukher Street 4, Kharkov 61002, Ukraine

Received 19 December 2003; accepted 25 March 2004

Abstract

New terbium complexes of derivatives of 2-oxo-4-hydroxy-quinoline-3-carboxylic acid are reported, which are highly luminescent, water soluble and do not require luminescence enhancers. The triplet-state energy levels of the ligands, the relative quantum yields (QYs) and the excitation maxima of the respective terbium chelates were determined. The large luminescence enhancement of one of these complexes by nucleic acids was investigated and a mechanism of its interaction with DNA is proposed. The optimal conditions for determination of DNA are equal concentrations of Tb^{3+} and ligand R_1 ($C = 1 \times 10^{-6}$ M), pH 9.0. Under optimal conditions the luminescence intensity (RI) is proportional to the concentration of fish sperm DNA (fsDNA) or calf thymus DNA (ctDNA), respectively, within the range of 0.05–1.5 μg ml^{-1}. The detection limits were 10 ng ml^{-1} for fsDNA and 12 ng ml^{-1} for ctDNA.

Keywords: Terbium complex; Nucleic acids; Luminescence; Intercalator

1. Introduction

Fluorescent probes including organic dyes [1–4], metal ions [5–7] and metal complexes [8,9] are frequently employed to investigate nucleic acids. In recent years, the use of coordination complexes of lanthanide ions as a probe to study nucleic acids has attracted much attention. Phenanthroline [10], diethylenetriaminepentaacetic acid and *p*-aminosalicylic acid [11], 1,6-bi(1′-phenyl-3′-methyl-5′-pyrazolone-4′-hexane-dione(BPMPHD)-cetyltrimethyl-ammonium bromide (CTMAB) [12], tetracycline [13], oxytetracycline [14] and tiron [15] are widely used as chelators.

Lanthanide complexes are used as probes and labels for direct determination of organic analytes, nucleic acids and in immunodiagnostic assays [16]. Their luminescence is the result of an efficient intramolecular energy transfer from the excited triplet-state of the ligand to the emitting level of the lanthanide [17]. These complexes show narrow emission bands, a large Stokes' shift and long luminescence decay times, which can be exploited to reduce interferences caused by a biological background [18]. General requirements for luminescent lanthanide chelates to be used as probes for bioassays include a high luminescence quantum yield, high kinetic stability and good water solubility.

We present here nine new terbium complexes of derivatives of 2-oxo-4-hydroxy-quinoline-3-carboxylic acid which are highly luminescent, have high stability and solubility in water and do not require the addition of luminescence enhancers such as micelles. These are the first terbium complexes based on quinolones for the luminescent determination of DNA. The complex showing the strongest luminescence enhancement upon interaction with nucleic acid was applied for a sensitive luminescent assay for the determination of DNA.

2. Experimental

2.1. Materials

Stock solutions of nucleic acids (0.1 mg ml^{-1}) were prepared by dissolving commercial fish sperm DNA (fsDNA)

* Corresponding author. Tel.: +49-941-943-4053; fax: +49-941-943-4064.
E-mail address: axel.duerkop@chemie.uni-regensburg.de (A. Duerkop).

1386-1425/$ – see front matter © 2004 Elsevier B.V. All rights reserved.
doi:10.1016/j.saa.2004.03.019

and calf thymus DNA (ctDNA) (Sigma, Steinheim, Germany) in 0.05 mM sodium chloride. Stock standard solutions (0.01 M) of terbium and aluminium chlorides were prepared by dissolving the corresponding terbium oxide or aluminium oxide (Sigma, 99.99%), respectively, in hydrochloric acid. Excess of HCl was evaporated to a wet residue and diluted with water. The metal concentration was determined by complexometric titration. Derivatives of 2-oxo-4-hydroxy-quinoline-3-carboxylic acid (R_1–R_9, see Table 1) were synthesized as described earlier [19].

Stock solutions (1×10^{-3} M) of these ligands were prepared by dissolving of accurately weighed preparations in water. Working solutions were prepared by appropriate dilution with water. A 0.1 M Tris–HCl buffer solution was prepared by dissolving 1.211 g of Tris base (USB, Cleveland, Ohio, USA) in 90 ml of water, adjusting the pH to 9.0 with HCl and making up the volume to 100 ml with water.

All chemicals used were of analytical grade. Doubly distilled water was used throughout.

2.2. Apparatus

Luminescence excitation and emission spectra were recorded on an Aminco-Bowman Series 2 luminescence spectrometer from SLM (Rochester, NY, USA). The spectrometer was equipped with a 150 W CW xenon lamp as excitation light source. The luminescence measurements described in Section 3.5. were obtained on an SDL-2 spectrofluorimeter (Leningrad Optomechanical Association, St. Petersburg, Russia). UV Spectra were recorded on a Cary 50 Bio spectrophotometer from Varian (Australia) and a Lambda-9 from Perkin–Elmer. The pH values were measured using an OP-211/1 laboratory digital pH-meter (Radelkis, Budapest, Hungary).

2.3. Procedures

To a 10 ml test tube, solutions of appropriate concentrations were added in the following order (in the absence and presence of nucleic acids): Tb^{3+} solution, R_x (ligand) solution, DNA solution and Tris–HCl buffer solution (pH 9.0). The mixture was diluted to 10 ml with water, stirred and allowed to stand for 10 min. The luminescence intensity (RI) was measured in a 1 cm quartz cell with an excitation wavelength of $\lambda_{ex} = 340$ nm and an emission wavelength of $\lambda_{em} = 545$ nm. All measurements were performed at room temperature. The enhanced relative luminescence intensity of Tb^{3+}–R_1 was calculated as $RI = RI' - RI_0$, where RI' and RI_0 are the relative luminescence intensities of the system with and without nucleic acid, respectively.

The triplet levels of the ligands were calculated from phosphorescence spectra of yttrium complexes of the ligands at 77 K. Quinine sulphate (Fluka, Buchs, Switzerland) was dissolved in 1 M H_2SO_4 to obtain a solution for quantum yield measurements. The luminescence quantum yields (QYs) were obtained by the method described by Haas and Stein [20] with quinine sulphate ($\Phi = 0.546$ in 1 M H_2SO_4 [21]) as quantum yield standard.

3. Results and discussion

3.1. Choice of ligands

It is common knowledge that ligands containing β-diketo groups efficiently coordinate to lanthanide ions since NMR-shift reagents like Eu(di-pivaloyl-methanate)$_3$ were introduced [22]. Quinolone based antibiotics like ciprofloxacine, norfloxacine, nalididxic acid and many others were often determined as luminescent β-diketo complexes with lanthanides. These quinolone derivatives were used alternatively for the determination of lanthanide ions [23]. To our best knowledge, we use quinolones for the determination of DNA, for the first time. For the luminescent detection of DNA we introduced a side chain containing a quaternary ammonium group to each ligand. This is needed for two reasons. One is to enable solubility of the complexes in aqueous buffers which are generally used in bioanalytics. The second is, that the luminescence enhancement of organic dyes like TOTO or TO-PRO and others was attributed to intercalation of the quaternary ammonium group into the grooves of DNA strands. We intended to use this group to attach the complex via the quinolone ligand to the DNA.

The ligand structure was varied using different ring structures 4-hydroxy-2-oxo-1,2-dihydro-3-quinolinecarboxamide, 6-hydroxy-4-oxo-1,2-dihydro-4H-pyrrolo[3,2,1-*ij*]quinoline-5-carboxamide and 7-hydroxy-5-oxo-2,3-dihydro-1H,5H-pyrido[3,2,1-*ij*]quinoline-6-carboxamide. Furthermore, the side chain attached to the 4-hydroxy-2-oxo-1,2-dihydro-3-quinolinecarboxamide part of the ligand was modified using ethyl, propyl and allyl chains. These ring and side chain parts of the ligand bind to the outer side of DNA whereas the ammonium group intercalates into the groove of the DNA strand. We intended to find a ligand ring structure which should be rigidized when the complex was bound to DNA. This improves the energy transfer from the ligand to the lanthanide ion and is accompanied by an increased quantum yield. Finally, the structure of the quaternary ammonium group was modified. This can determine how deep the ligand intercalates into the DNA groove. This influences the rigidization of the whole complex in bound state, again, and is therefore another means to control the quantum yield.

3.2. Spectral characteristics

The absorption spectra of the ligands in aqueous solutions are characterized by the presence of two bands in the UV (Table 2). The high molar extinction coefficients of these bands enable effective absorption of excitation light energy. The triplet energy levels of the ligands are between 20800 and 22250 cm^{-1}. The ligands can transfer energy to the

Table 1
Structural formulae and names of the ligands investigated

N	Structure and name
R_1	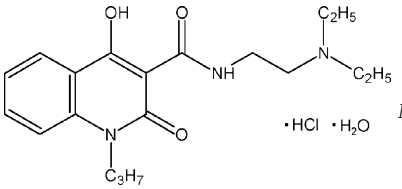 *N*-[2-(diethylamino)ethyl]-4-hydroxy-2-oxo-1-propyl-1,2-dihydro-3-quinolinecarboxamide
R_2	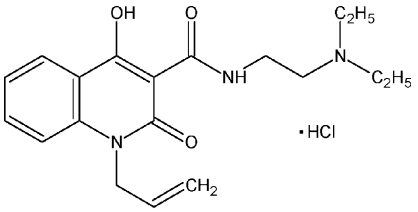 1-allyl-*N*-[2-(diethylamino)-ethyl]-4-hydroxy-2-oxo-1,2-dihydro-3-quinolinecarboxamide
R_3	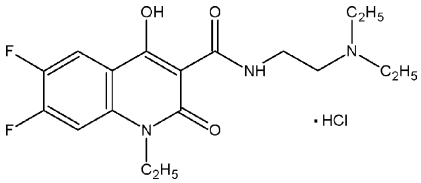 *N*-[2-(diethylamino)ethyl]-1-ethyl-6,7-difluoro-4-hydroxy-2-oxo-1,2-dihydro-3-quinolinecarboxamide
R_4	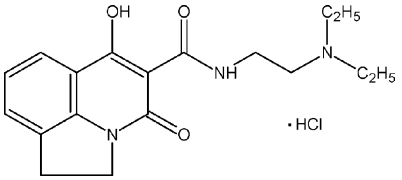 *N*-[2-(diethylamino)ethyl]-6-hydroxy-4-oxo-1,2-dihydro-4H-pyrrolo[3,2,1-*ij*]quinoline-5-carboxamide
R_5	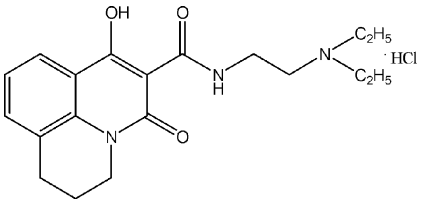 *N*-[2-(diethylamino)ethyl]-7-hydroxy-5-oxo-2,3-dihydro-1H,5H-pyrido[3,2,1-*ij*]quinoline-6-carboxamide
R_6	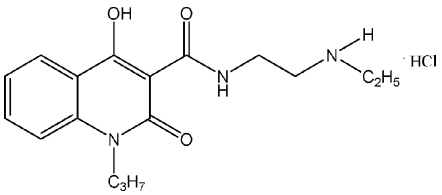 *N*-[2-(ethylamino)ethyl]-4-hydroxy-2-oxo-1-propyl-1,2-dihydro-3-quinolinecarboxamide
R_7	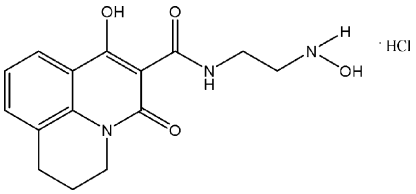 7-hydroxy-*N*-[2-(hydroxyamino)ethyl]-5-oxo-2,3-dihydro-1H,5H-pyrido[3,2,1-*ij*]quinoline-6-carboxamide
R_8	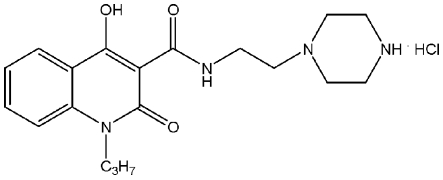 4-hydroxy-2-oxo-*N*-[2-(1-piperazinyl)ethyl]-1-propyl-1,2-dihydro-3-quinolinecarboxamide

Table 1 (*Continued*)

N	Structure and name
R_9	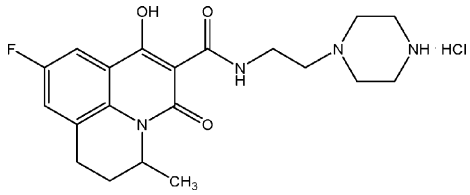 9-fluoro-7-hydroxy-3-methyl-5-oxo-*N*-[2-(1-piperazinyl)ethyl]-2,3-dihydro-1H, 5H-pyrido[3,2,1-*ij*]quinoline-6-carboxamide

centre ion only, if their triplet energy level is higher than that of the lanthanide ion. All ligands fulfil this requirement because the triplet energy level of Tb^{3+} ($^5D_4$) is located at 20500 cm^{-1}.

It is obvious from Table 2, that the differences of triplet-state energies of the ligands are too small to be attributed to changes of their structure. This is also true for the variations of the molar absorbances and absorption maxima.

The excitation and emission spectra of Tb^{3+} complexes R_1–R_9 were recorded. Fig. 1 (left) shows the excitation spectrum of the Tb^{3+}–R_1 complex monitored at 545 nm. The excitation maximum is at 309 nm which is similar to the other complexes (see Table 2). The emission bands of the Tb^{3+}–R_1 complex (Fig. 1, right) are located at 490, 545, 585 and 620 nm generated from the $^5D_4 \rightarrow {}^7F_6$, $^5D_4 \rightarrow {}^7F_5$, $^5D_4 \rightarrow {}^7F_4$ and $^5D_4 \rightarrow {}^7F_3$ transitions of Tb^{3+}, respectively. The maxima of the emission bands of all nine complexes do not vary in wavelength but in intensity. Especially the 545 nm bands are hypersensitive to the molecular environment of the respective complex. Therefore, the changes of the luminescence intensity of this band are most often used for analytical applications with Tb^{3+} complexes.

Table 2
Triplet-state energy levels (E), absorption maxima (λ_{abs}) with molar absorbances (ϵ) of ligands R_1–R_9; quantum yields (Φ) and excitation maxima (λ_{ex}), of the Tb complexes with these ligands

Ligand	E (cm^{-1})	λ_{abs} (nm)	ε ($l\,M^{-1}\,cm^{-1}$)	Φ	λ_{ex} (nm)
1	22100	290 238	25600 73300	0.40	309
2	22250	290 238	25800 69100	0.32	322
3	22200	296 231	20500 64800	0.25	310
4	21050	292 246	23400 53800	0.23	312
5	21740	292 237	26000 64000	0.38	309
6	22200	290 238	29300 87800	0.24	316
7	21500	292 237	31800 79300	0.37	317
8	21740	291 238	18100 52400	0.36	315
9	20830	292 236	26600 63300	0.39	319

The quantum yields of complexes Tb^{3+} with R_1–R_9 were measured in Tris–HCl buffer (pH 9.0) relative to quinine sulphate at λ_{ex} = 340 nm. The quantum yields (QYs) of the Tb^{3+} chelates with R_1–R_9 are given in Table 2 and vary from 0.23 to 0.40. From the structures displayed in Table 1, it is obvious that the 7-hydroxy-5-oxo-2,3-dihydro-1H,5H-pyrido[3,2,1-*ij*] quinoline-6-carboxamides R_5, R_7 and R_9 display high QYs. This is independent from the different groups attached to the ammonium moiety of these ligands. The 4-hydroxy-2-oxo-1,2-dihydro-3-quinolinecarboxamide structures R_1 and R_8 can also show high quantum yields upon complexation with Tb^{3+}. But here, a propyl side chain seems to be a prerequisite for high QYs, because the complexes without this chain (R_2 and R_3) display significantly lower quantum yields. On comparing the QYs of R_1 and R_8 it is obvious that the structure of the different groups attached to the ammonium moiety has only minor influence on the energy transfer from ligand to the centre ion. The 6-hydroxy-4-oxo-1,2-dihydro-4H-pyrrolo[3,2,1-*ij*] quinoline-5-carboxamide structure has the lowest QY and seems not very suitable for luminescent determination of DNA. As can be seen from Table 2, Tb^{3+}–R_1 has the highest quantum yield. Therefore, this complex was the preferred candidate for the luminescent determination of DNA.

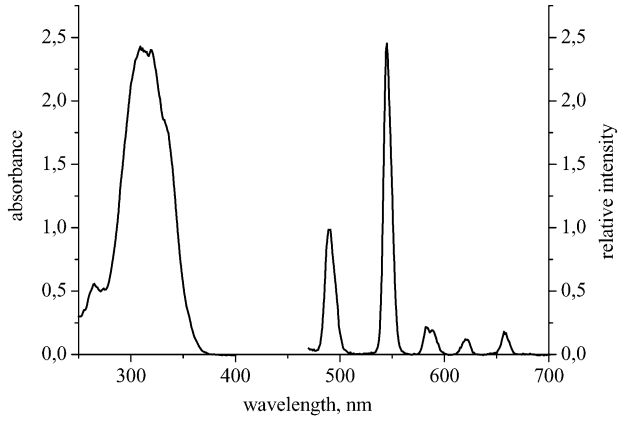

Fig. 1. Excitation and emission spectra of Tb^{3+}–R_1 complex ($C_{Tb^{3+}} = 1 \times 10^{-6}$ M; $C_{R_1} = 2 \times 10^{-6}$ M; pH 9.0; λ_{ex} = 340 nm and λ_{em} = 545 nm).

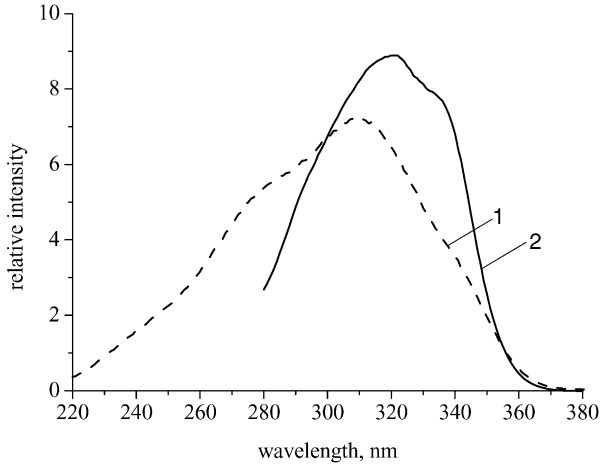

Fig. 2. Excitation spectrum of Tb^{3+}–R_1 in absence and presence of DNA. $C_{Tb^{3+}} = 1 \times 10^{-6}$ M; $C_{R_1} = 1 \times 10^{-6}$ M; $C_{fsDNA} = 0.5\,\mu g\,ml^{-1}$; pH 9.0; $\lambda_{em} = 545$ nm (1: Tb^{3+}–R_1; 2: Tb^{3+}–R_1–fsDNA).

The luminescence of all Tb^{3+}-complexes in absence and in presence of $0.5\,\mu g\,ml^{-1}$ fsDNA was investigated. This was done to determine the dynamic range of the luminescence enhancement upon binding to DNA. Here, the Tb^{3+}–R_1 complex displays the most pronounced luminescence enhancement compared to the other complexes. Therefore Tb^{3+}–R_1 complex was used for further experiments with DNA. The excitation maximum of the Tb^{3+}–R_1–DNA complex is increased and red shifted by 10 nm compared to Tb^{3+}–R_1 complex (Fig. 2). This indicates the interaction between Tb^{3+}–R_1 complex and nucleic acid. The luminescence spectra of Tb^{3+}–R_1–DNA complex are similar to those of Tb^{3+}–R_1, but the luminescence intensity is greatly enhanced upon addition of nucleic acid (see Section 3.4).

3.3. Effect of pH, stoichiometry and buffer composition

The luminescence intensity of Tb^{3+}–R_1–fsDNA is strongly dependent of pH (Fig. 3). It can be seen from Fig. 3

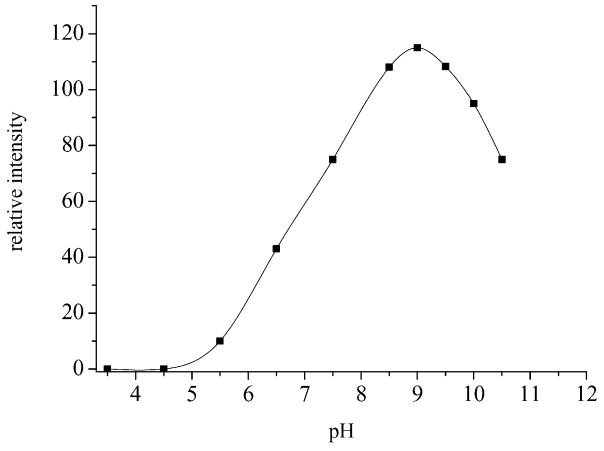

Fig. 3. Dependence of RI of Tb^{3+}–R_1–fsDNA complex of the pH ($C_{Tb^{3+}} = 1 \times 10^{-6}$ M; $C_{R_1} = 1 \times 10^{-6}$ M; $C_{fsDNA} = 0.5\,\mu g\,ml^{-1}$).

that the maximum luminescence intensity of the system is reached at pH 9.0. This is in accordance with the fact that the ligand will coordinate with Tb^{3+} more efficiently in its enolic form. Therefore, we choose pH 9.0 (0.1 M Tris–HCl buffer) for the further experiments.

Tb^{3+} forms complexes with R_1–R_9 in a 1:2 ratio. This was determined by the molar ratio method. The influence of the Tb^{3+} concentration on the luminescence intensity was investigated in the concentration range of 5×10^{-7} M to 5×10^{-6} M of Tb^{3+} with $0.50\,\mu g\,ml^{-1}$ of fsDNA and 1×10^{-6} M of R_1 in Tris–HCl buffer (pH 9.0). The influence of R_1 concentration on the luminescence intensity was investigated at constant Tb^{3+}concentration of 1×10^{-6} M. The optimal conditions were equal concentrations of Tb^{3+} and R_1 ($C = 1 \times 10^{-6}$ M) which were chosen for further experiments.

It is well known that the addition of solvents, various surfactants and synergetic agents (trioctylphosphinoxide/TOPO) are the prerequisites for lanthanide luminescence to be enhanced [12]. The influence of various solvents was investigated. The maximum luminescence intensity was observed in Tris-buffered solution. Luminescence quenching was observed in 50% (v/v) mixtures of water with various solvents in the following order: methanol, ethanol, dimethylformamide, dimethylsulfoxide (20–25% luminescence decrease for each mixture); acetone, iso-propanol (50% luminescence decrease for each mixture). It was found as well that the effect of cationic, anionic and non-ionic surfactants, respectively, and a synergetic agent (TOPO) on the luminescence intensity is insignificant. This is a major advantage compared to all lanthanide based methods mentioned in Table 3 because the addition of the enhancer always elongates the time for the determination of the sample and causes higher costs for the additional reagent. All effects mentioned above are typical for Tb^{3+}–R_1 and Tb^{3+}–R_1–DNA complexes.

Table 3
Common luminescence probes for nucleic acid determination

Luminescence probe	Nucleic acid	LOD ($ng\,ml^{-1}$)	Reference
Ethidium bromide	nDNA	10	[1]
Hoechst 33258	nDNA	10	[2]
Methylene blue	nDNA	28	[3]
Vitamin K_3	nDNA, RNA	10, 26	[4]
Tb^{3+}	RNA	100	[5,6]
Tb-1,10-phenanthroline	dDNA, RNA	100	[10]
Eu-tetracycline	nDNA	10	[13]
La-8-hydroxyquinoline	ctDNA, fsRNA	76, 68	[8]
Al-8-hydroxyquinoline	ctDNA, fsRNA	24, 13	[9]
Tb-BPMPHD-CTMAB	nDNA	9	[12]
Eu-oxytetracycline	nDNA	11	[14]
PicoGreen	dsDNA	0,25	[27]
OliGreen	ssDNA	0,1	[27]
RiboGreen	RNA	1	[27]
Tb^{3+}–R_1	ctDNA	10	
Tb^{3+}–R_1	fsDNA	12	

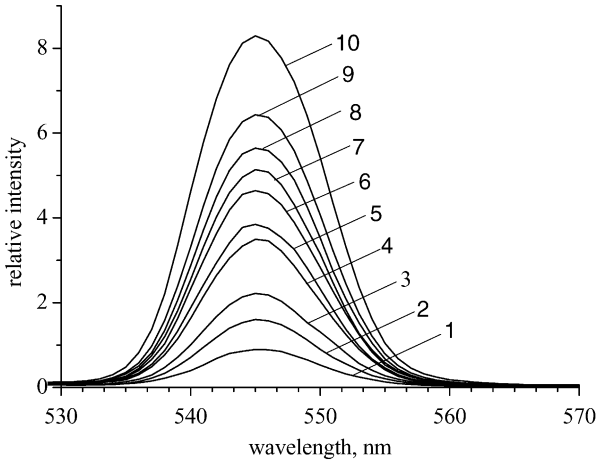

Fig. 4. Luminescence enhancement of Tb^{3+}–R_1 complex upon addition of various concentrations of fsDNA ($C_{Tb^{3+}} = 1 \times 10^{-6}$ M; $C_{R_1} = 1 \times 10^{-6}$ M; pH 9.0; $\lambda_{ex} = 340$ nm and $\lambda_{em} = 545$ nm); C_{fsDNA}, $\mu g\,ml^{-1}$ (curve number): 0 (1); 0.05 (2); 0.1 (3); 0.4 (4); 0.5 (5); 0.7 (6); 0.8 (7); 0.9 (8); 1.0 (9); 1.5 (10).

3.4. Luminescence determination of DNA

The luminescence enhancement of the Tb^{3+}–R_1 complex was studied within a concentration range of 0.05–1.5 $\mu g\,ml^{-1}$ of both, fsDNA and ctDNA. The emission spectra of the corresponding luminescence titration of Tb^{3+}–R_1 with fsDNA are shown in Fig. 4. A strong, up to eight-fold enhancement of the luminescence intensity is observed.

Linear calibration plots were established from the spectra for both, fsDNA and ctDNA. The regression data and LODs (3σ/slope) are given in Table 4. A good agreement between data and calibration plot can be seen from Fig. 5 for Tb^{3+}–R_1 with fsDNA. The calibration plots are almost identical for fsDNA and ctDNA. Therefore, only the data for the calibration with fsDNA is shown in Fig. 5. The limit of detection was 0.010 $\mu g\,ml^{-1}$ for fsDNA and 0.012 $\mu g\,ml^{-1}$ for ctDNA.

A comparison of the sensitivities of Tb^{3+}–R_1 and other common probes for nucleic acid detection is given in Table 3. Tb^{3+}–R_1 displays comparable sensitivity to ethidium bromide (EB), however it is not cancerogenic. Furthermore, the large Stokes' shift of Tb-complexes facilitates the separation of the excitation and emission light which is particularly important in filter-based instruments like microtiterplate readers. The long luminescence decay times of Tb^{3+} complexes offer gated detection as a further detection method which is

Table 4
Analytical parameters for DNA determination

DNA	Linear range ($\mu g\,ml^{-1}$)	Correlation coefficient	Detection limit ($\mu g\,ml^{-1}$)
fsDNA	0.05–1.50	0.991	0.010
ctDNA	0.05–1.50	0.989	0.012

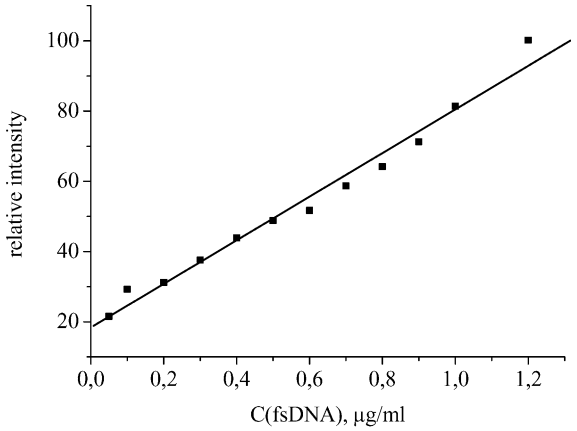

Fig. 5. Calibration graph for the determination of fsDNA ($C_{Tb^{3+}} = 1 \times 10^{-6}$ M; $C_{R_1} = 1 \times 10^{-6}$ M; pH 9.0; $\lambda_{em} = 545$ nm).

not disturbed by fluorescence of a short-lived (up to 20 ns) biological background. The longer lifetime of terbium complexes compared to europium complexes enables sensitive detection even with very simple equipment for measurement of luminescence decay times. This will be the subject of further research to improve the LODs.

We use an excitation wavelength of 340 nm which is not in the UV compared to the 267 and 265 nm of the two complexes employing the luminescence of 8-hydroxyquinoline [8,9]. The detection wavelength of 545 nm of our method is also more longwave than the 485 nm of others [8,9]. This improves the signal-to-noise ratio of the detection because in bioanalysis background fluorescence is significantly decreased at longwave excitation and detection wavelengths.

3.5. The interaction mechanism of Tb^{3+}–R_1 with nucleic acid

From the luminescence data presented in Fig. 5, binding constants were calculated [24] to be ($\log k = 6.9 \pm 0.5$). This value is typical for intercalating organic dyes. To confirm the assumption of intercalation, we used the ethidium bromide displacement assay. However, the overlap of the emission band of Eu(III) ($^5D_0 \rightarrow {}^7F_1$, $\lambda = 590$ nm), which was present in terbium oxide in amounts of about 1×10^{-3}%, with the emission band of the ethidium bromide ($\lambda = 595$ nm) prevented to choose Tb^{3+}–R_1 for the displacement assay. Fortunately, the intercalation characteristics of aluminium complexes are close to those of terbium. Therefore, it is possible to infer from data of the complex of R_1 with Al^{3+} to similar properties of Tb^{3+}–R_1. This approach was used in an experiment of the ethidium bromide displacement with the non-luminescent Al^{3+}–R_1 complex. In case the investigated complex is an intercalator, it is able to displace ethidium bromide from its complex with DNA. The luminescence intensity of the whole system will then be proportional to the amount of ethidium bromide which is bound to DNA. Therefore, the luminescence intensity is

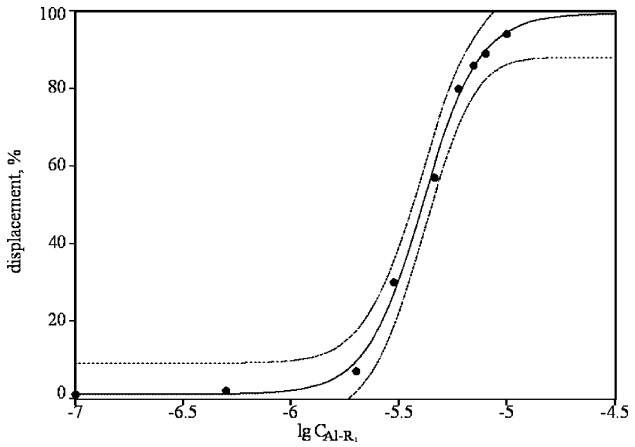

Fig. 6. Ethidium bromide displacement (%) by Al^{3+}–R_1 complex in semi-logarithmic representation of C(Al^{3+}–R_1).

reduced on addition of Al^{3+}–R_1 to the solution containing EB and DNA.

The C_{50} value is defined as the concentration of the complex reducing the luminescence of the DNA-bond ethidium bromide by 50%. It was determined from the value of the abscissa inflection of the sigmoid curve in $\log C_{Al^{3+}–R_1}$ of the EB displacement percent coordinates (Fig. 6). Binding constants were calculated from the C_{50} values using the formula [25]

$$K_{Al^{3+}–R_1} = \left(\frac{C_{EB}}{C_{50(Al^{3+}–R_1)}}\right) \times K_{EB};$$

($K_{EB} = 1 \times 10^7\ M^{-1}$).

The luminescence intensity of the peaks of EB (relative control) at 595 nm (excitation at 365 nm) in a series of solutions containing DNA ($C_{DNA} = 1\,\mu M$), sodium azide ($C_{NaN_3} = 0.3$ mM), EB ($C_{EB} = 0.5\,\mu M$) and Al^{3+}–R_1 in various concentrations within a range 1×10^{-7} M to -1×10^{-5} M were measured. A solution free of the investigated complex was used as control. The obtained value of the binding constant ($\log k = 6.1 \pm 0.4$) is typical for mono-intercalators into DNA [26] and is close to the value of the constant obtained by a luminescence titration.

We suppose that side chain fragments of R_1 interact with the grooves of DNA due to the formation of hydrogen bonds between non-divided electron pairs of nitrogen atoms of DNA base pairs and the $–N^+(C_2H_5)_2H$ group of the complex. This interaction leads to significant ordering and reduction of non-radiative energy losses and, as a result, the luminescence intensity is increased upon binding with DNA.

4. Conclusions

Nine quinolones were used as ligands for new terbium complexes for the luminescent determination of DNA. The ligand structure was optimized to obtain high quantum yields and a large signal enhancement upon binding to DNA. The complexes are water soluble, not cancerogenic and display favourably long Stokes' shifts and high quantum yields. Unlike other methods employing lanthanide complexes for DNA determination, the addition of surfactants or luminescence enhancers is not required. The long luminescence decay times allow additional detection schemes like gated measurements in microplate readers to enhance sensitivity by off-gating of short-lived background luminescence. Complex Tb^{3+}–R_1 was chosen for the luminescent determination of DNA. An up to 10-fold luminescence enhancement of this terbium complex upon titration with DNA was observed. The optimal conditions are equal concentrations of Tb^{3+} and ligand R_1 ($C = 1 \times 10^{-6}$ M) at pH 9.0. Under these conditions, the luminescence intensity is linearly dependent on the concentration of fsDNA and ctDNA within the range of 0.05–1.5 $\mu g\,ml^{-1}$. The detection limits are 10 $ng\,ml^{-1}$ for fsDNA and 12 $ng\,ml^{-1}$ for ctDNA, respectively. The binding constant of Tb^{3+}–R_1 to DNA was determined to be $\log k = 6.1$ by both, luminescence titration and ethidium bromide displacement assay.

References

[1] J.B. Lepecq, C. Paoletti, Anal. Biochem. 17 (1966) 100–107.
[2] C. Labara, K. Paigen, Anal. Biochem. 102 (1980) 344–352.
[3] W.Y. Li, J.G. Xu, X.Q. Guo, Q.Z. Zhu, Y.B. Zhao, Anal. Lett. 30 (1997) 527–536.
[4] W.Y. Li, J.G. Xu, X.Q. Guo, Q.Z. Zhu, Y.B. Zhao, Anal. Lett. 30 (1997) 245–257.
[5] S. Sueda, T. Ihara, B. Juskowiak, M. Takagi, Anal. Chim. Acta 365 (1998) 27–31.
[6] J.H. Yang, C.L. Tong, N.Q. Jie, H.Y. Gong, Chin. Biochem. J. 12 (1996) 143–146.
[7] M.D. Topal, J.R. Fresco, Biochemistry 19 (1980) 5531–5537.
[8] C.Z. Huang, K.A. Li, S.Y. Tong, Anal. Lett. 29 (1996) 1705–1717.
[9] C.Z. Huang, K.A. Li, S.Y. Tong, Anal. Lett. 30 (1997) 1305–1319.
[10] Y.X. Ci, Y.Z. Li, W.B. Chang, Anal. Chim. Acta 248 (1991) 589–594.
[11] S.S. Saavedra, E.G. Picozza, Analyst 114 (1989) 835–841.
[12] X. Wu, J. Yang, F. Huang, M. Wang, L. Sun, G. Xu, Anal. Lett. 32 (1999) 2417–2425.
[13] Y.X. Ci, Y.Z. Lu, X.J. Liu, Anal. Chem. 67 (1995) 1785–1788.
[14] R. Liu, J. Yang, X. Wu, J. Lumin. 96 (2002) 201–209.
[15] Y.-B. Zhao, D.-Y. Wang, X.-Q. Guo, J.-G. Xu, Anal. Chim. Acta 353 (1997) 329–335.
[16] K. Blomberg, P. Hurskainen, I. Hemilla, Clin. Chem. 45 (1999) 855–861.
[17] F.S. Richardson, Chem. Rev. 82 (1982) 541–552.
[18] P.R. Selvin, in: W. Rettig, B. Strehmel, S. Schrader, H. Seifert (Eds.), Applied Luminescence in Chemistry, Biology and Medicine, Springer, Berlin, 1998, p. 457.
[19] I.V. Ukrainets, D.N. Amin, I.V. Gorlacheva, O.V. Gorokhova, L.V. Sidorenko, A.V. Turov, Chem. Heterocycl. Compd. 2 (2000) 207–211.
[20] Y. Haas, G. Stein, J. Phys. Chem. 75 (1971) 3668–3677.

[21] S.R. Meech, D. Phillips, J. Photochem. 23 (1983) 193–198.
[22] C.C. Hinckley, J. Am. Chem. Soc. 91 (1969) 5160–5162.
[23] A. Gómes-Hens, M.P. Aguilar-Caballos, Trends Anal. Chem. 21 (2002) 131–141.
[24] C.V. Kumar, E.H. Asuncion, J. Am. Chem. Soc. 115 (1993) 8547–8551.
[25] I. Antonini, P. Polucci, L.R. Kelland, J. Med. Chem. 42 (1999) 2535–2541.
[26] H. Lyakhova, S. Lyakhov, L. Litvinova, Z. Topilova, I. Velcheva, Khim.-Pharm. Zhurn. 37 (2003) 16–21.
[27] R.P. Haugland (Ed.), Handbook of Fluorescent Probes and Research Products, 9th ed., Molecular Probes, 2003, pp. 301–304.